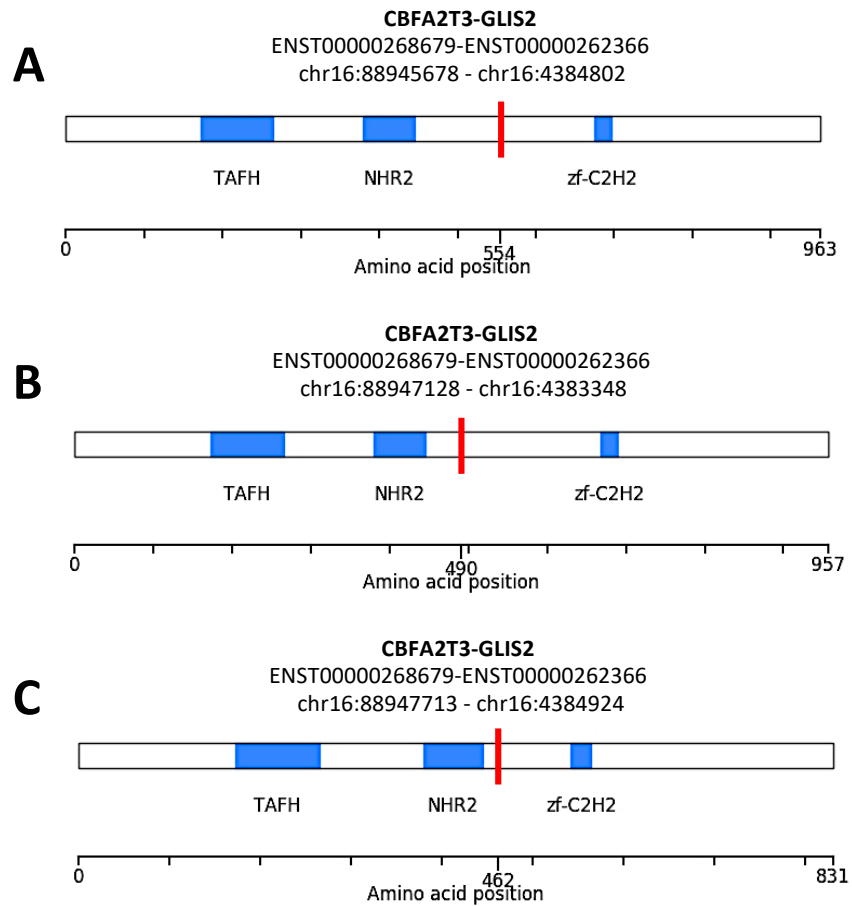


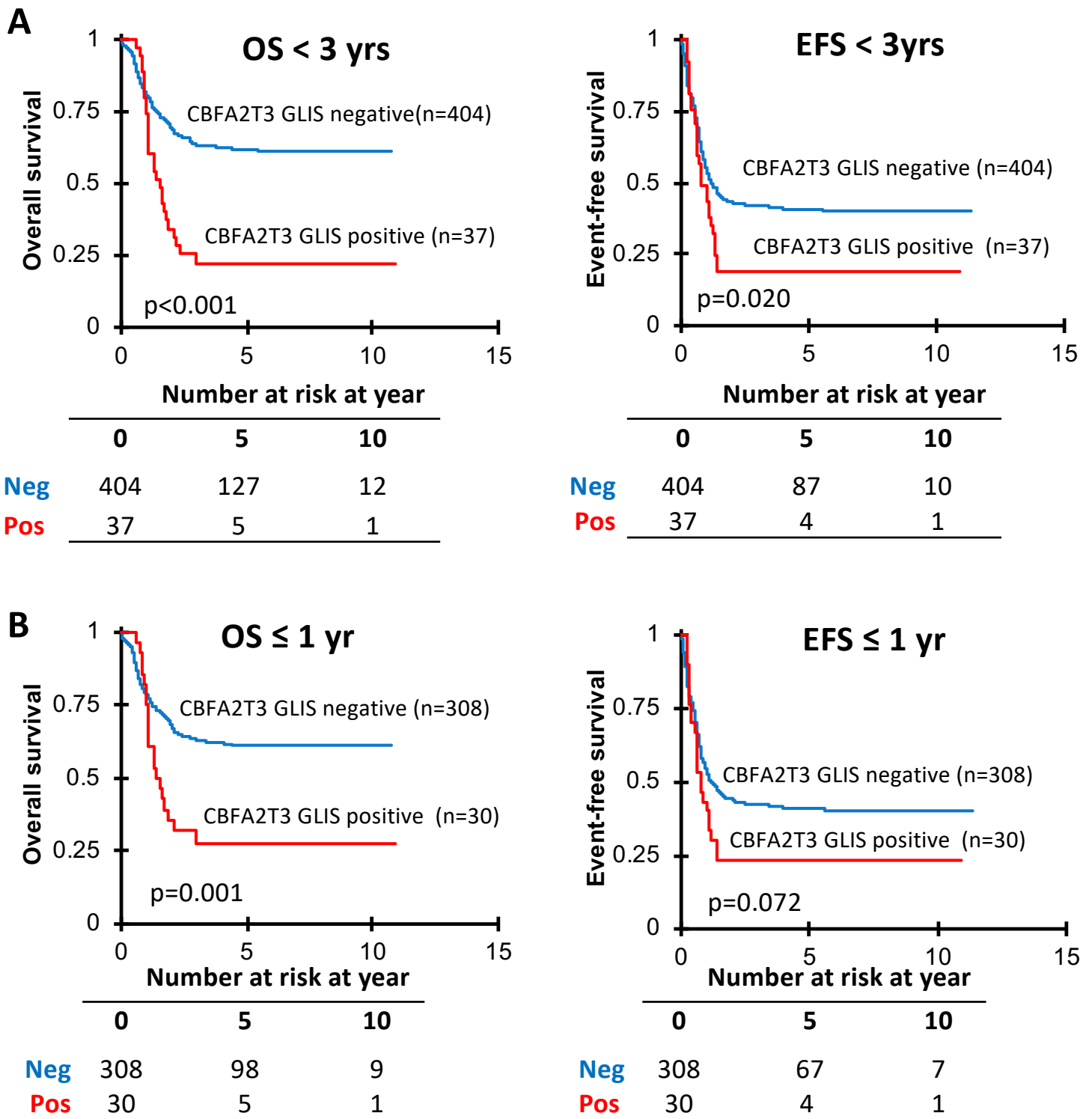
**Comprehensive Transcriptome Profiling of Cryptic  
*CBFA2T3-GLIS2* Fusion-positive AML Defines Novel  
Therapeutic Options – A COG and TARGET  
Pediatric AML Study**

# Supplemental Figures

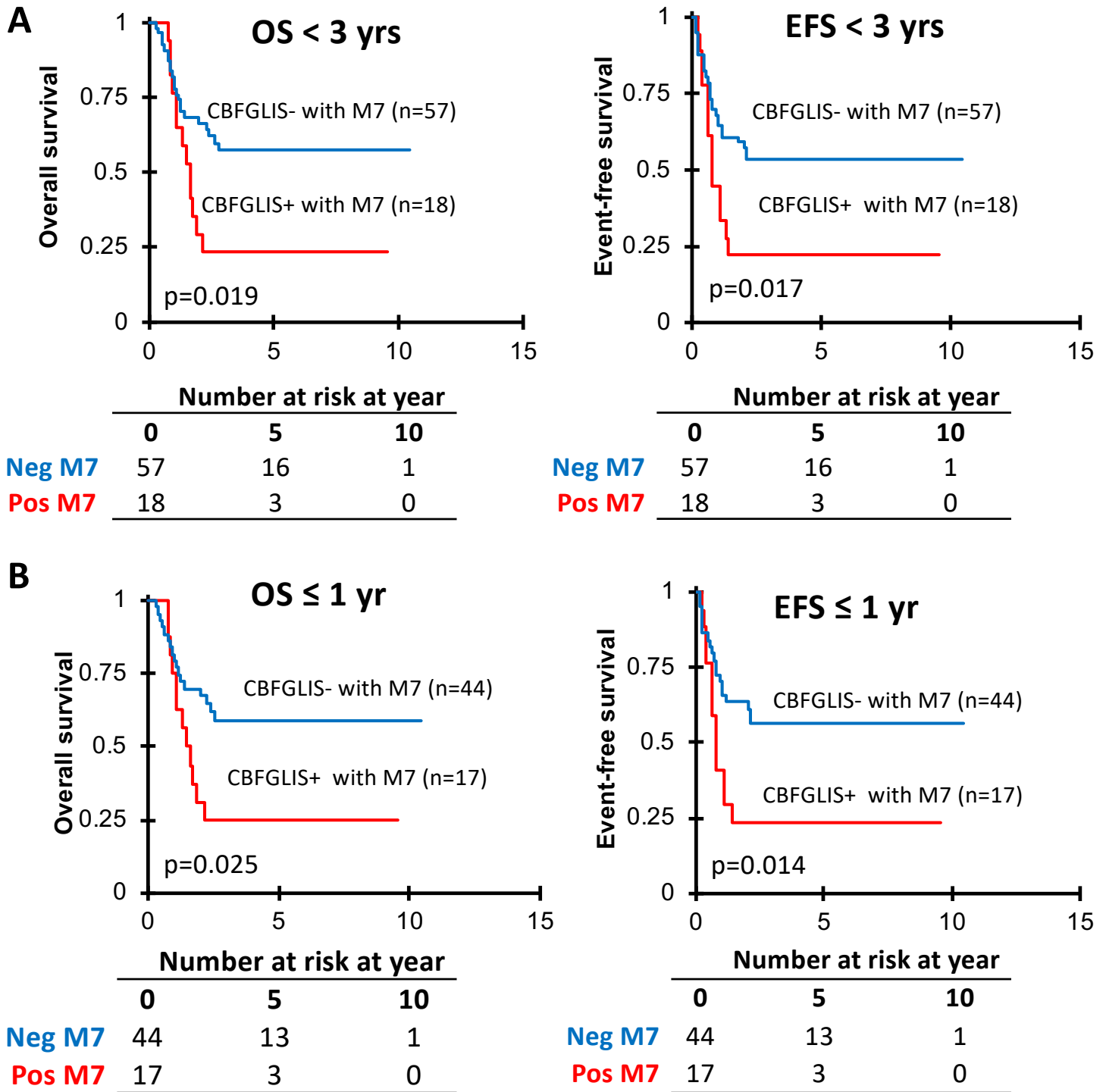
Smith, J., L., Ries, R.,E., ... Meshinchi, S.



**Supplemental Figure 1. Schematic of fusion proteins for each unique *CBFA2T3-GLIS2* breakpoint detected by RNA-sequencing. A) The most common breakpoint and B-C) the two non-typical breakpoints detected are represented. The breakpoint position is denoted by the red vertical line.**



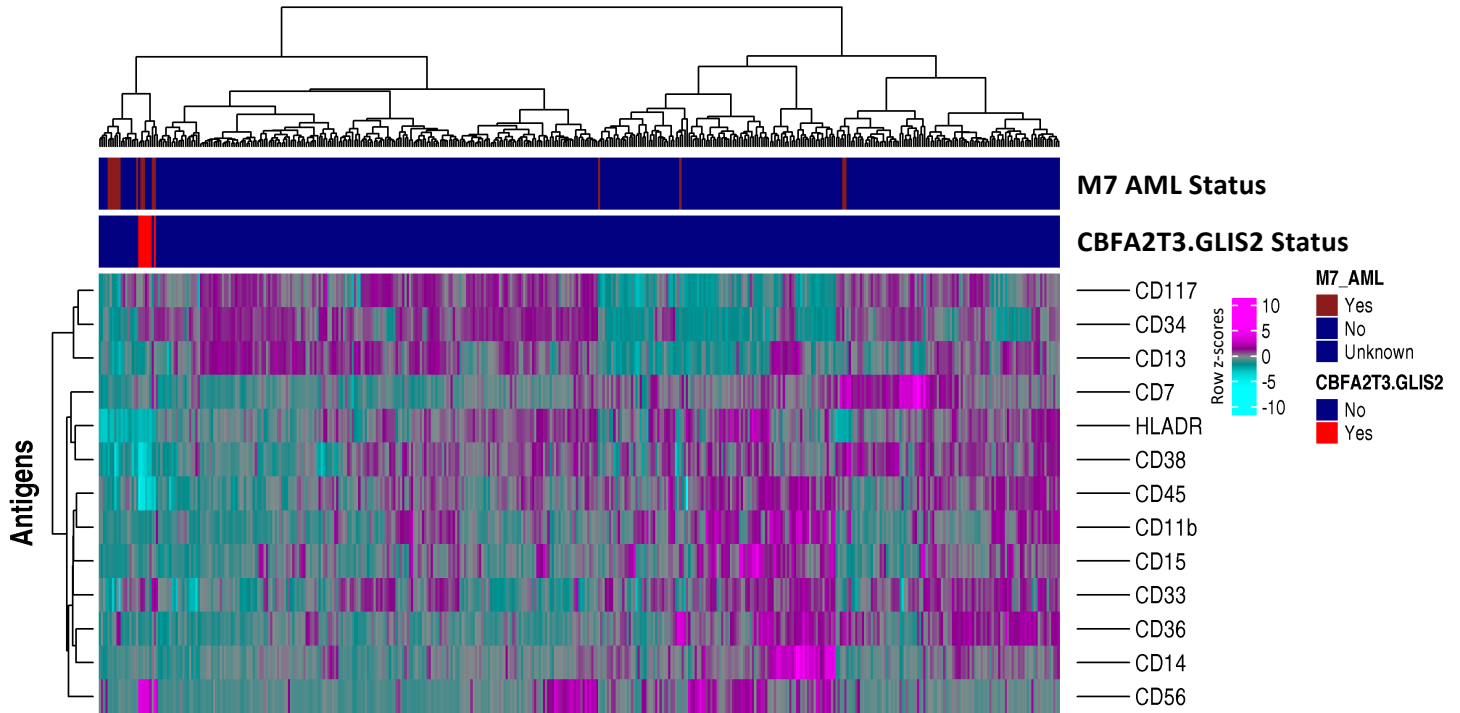
**Supplemental Figure 2. Overall Survival and Event-free survival in infant AML with and without the *CBFA2T3-GLIS2* Fusion. A)** Kaplan-Meier curves demonstrating *CBFA2T3-GLIS2* AML patients (< 3 years old) have an adverse outcome compared to fusion-negative cohorts who are < 3 years old and **B)** similarly, *CBFA2T3-GLIS2* who are  $\leq$  1 year old compared to age matched heterogenous fusion negative population.



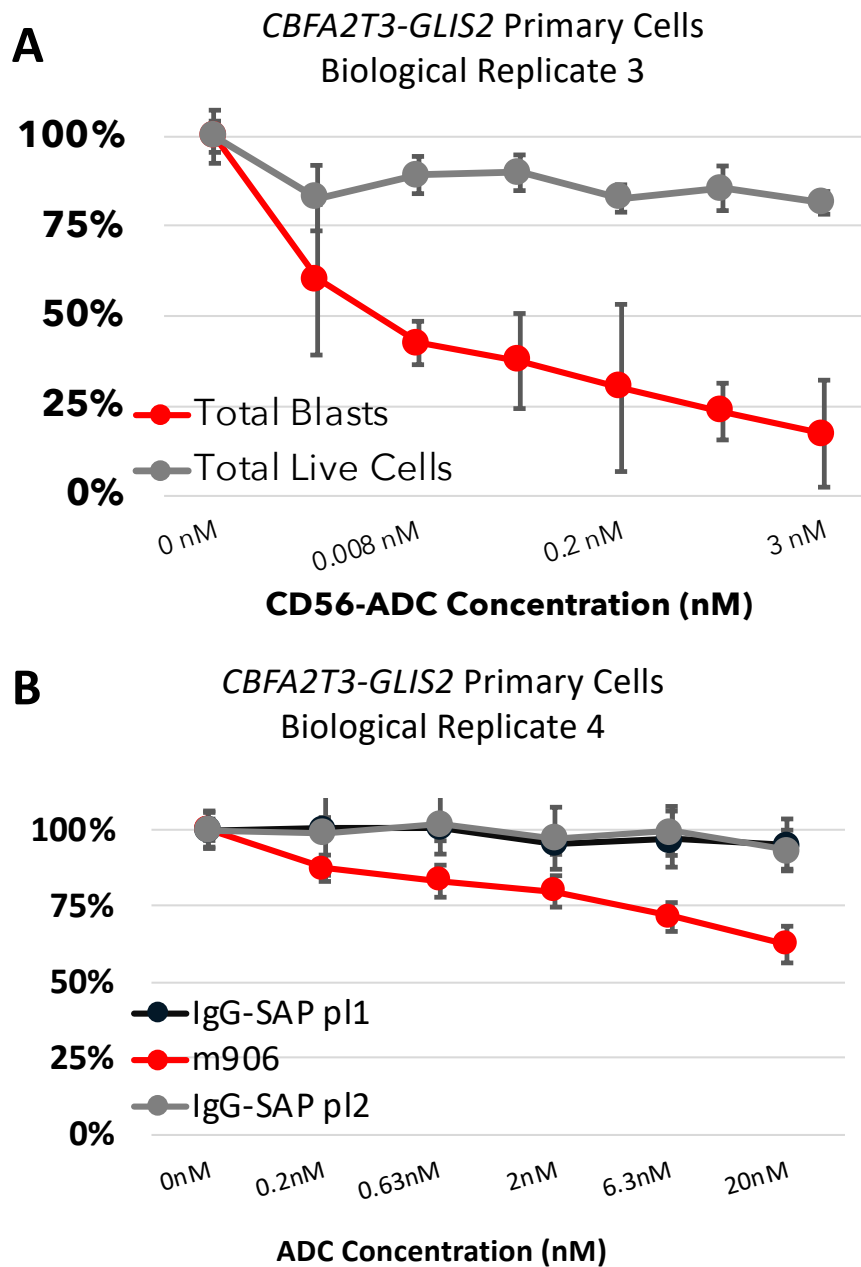
**Supplemental Figure 3. Overall Survival and Event-free survival in infant M7 (megakaryoblastic) AML with and without the *CBFA2T3-GLIS2* Fusion. A) Kaplan-Meier curves demonstrating M7 *CBFA2T3-GLIS2* AML patients (< 3 years old) have an adverse outcome compared to fusion-negative M7 cohorts of the same age. B) *CBFA2T3-GLIS2* cases ≤ 1 year old who have M7 morphology have poor outcomes for OS and EFS compared to heterogenous M7 fusion-negative patients.**



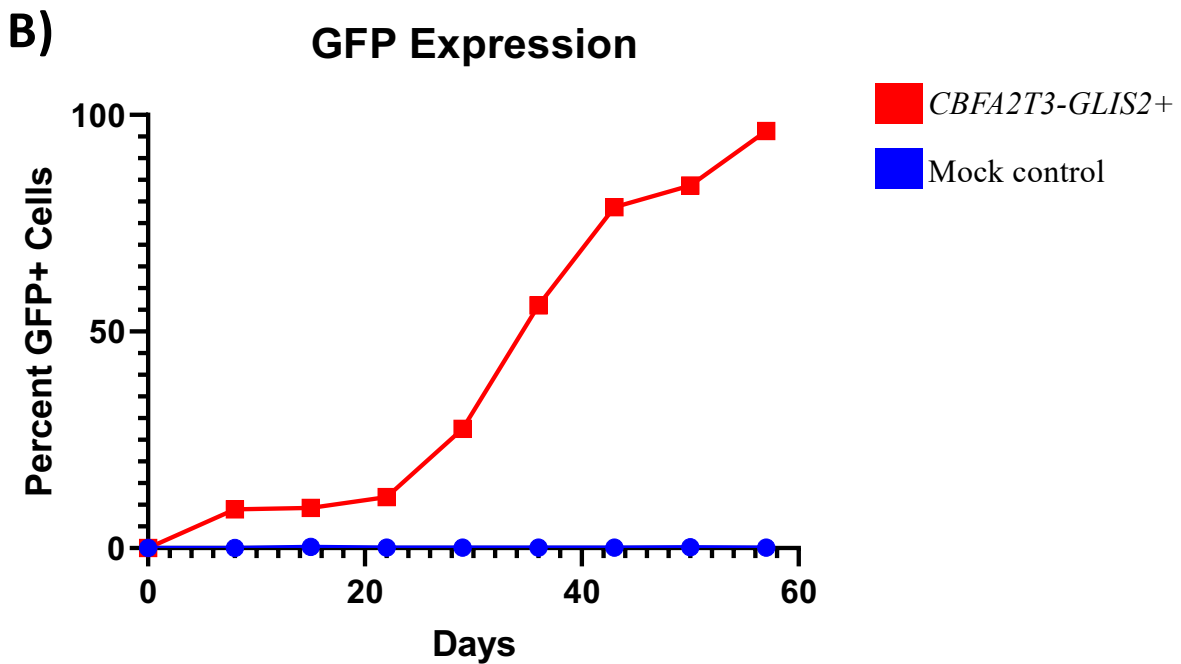
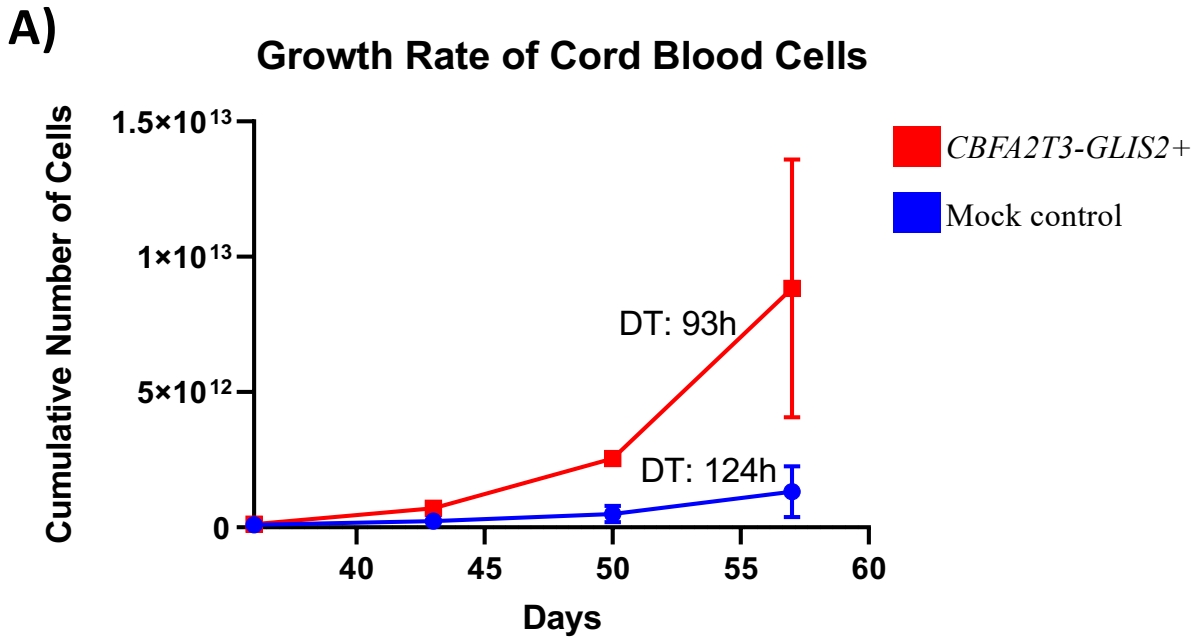
### Cell-Surface Antigen Expression in *CBFA2T3-GLIS2* AML



**Supplemental Figure 4. Fusion-positive cases display a unique immunophenotype.** Unsupervised hierarchical clustering of mean fluorescent intensity (MFI) values from 13 cell surface antigens in the pediatric AML cohort AAML0531 (N = 437). *CBFA2T3-GLIS2* AML (N=7) cluster closely together and exhibit high expression of CD56, and dim to absent expression of HLADR, CD38, and CD45, a pattern representative of RAM phenotype.

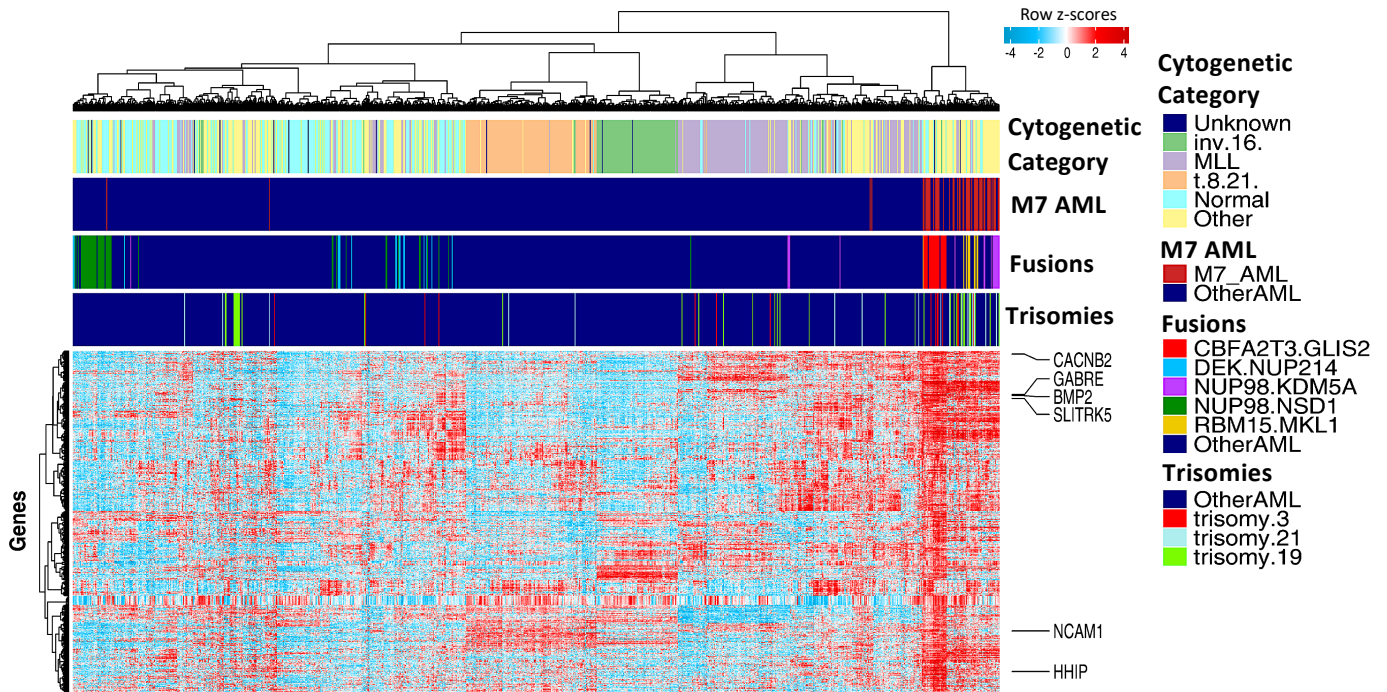


**Supplemental Figure 5. The CD56 anti-body drug conjugate (ADC) exhibits potent cytotoxicity.** **A)** An additional *CBFA2T3-GLIS2* patient primary sample exposed to varying concentrations of the CD56-ADC. **B)** Cytotoxicity assay with *CBFA2T3-GLIS2* primary cells exposed CD56-ADC or the non-targeting conjugate control, IgG-SAP ADC.

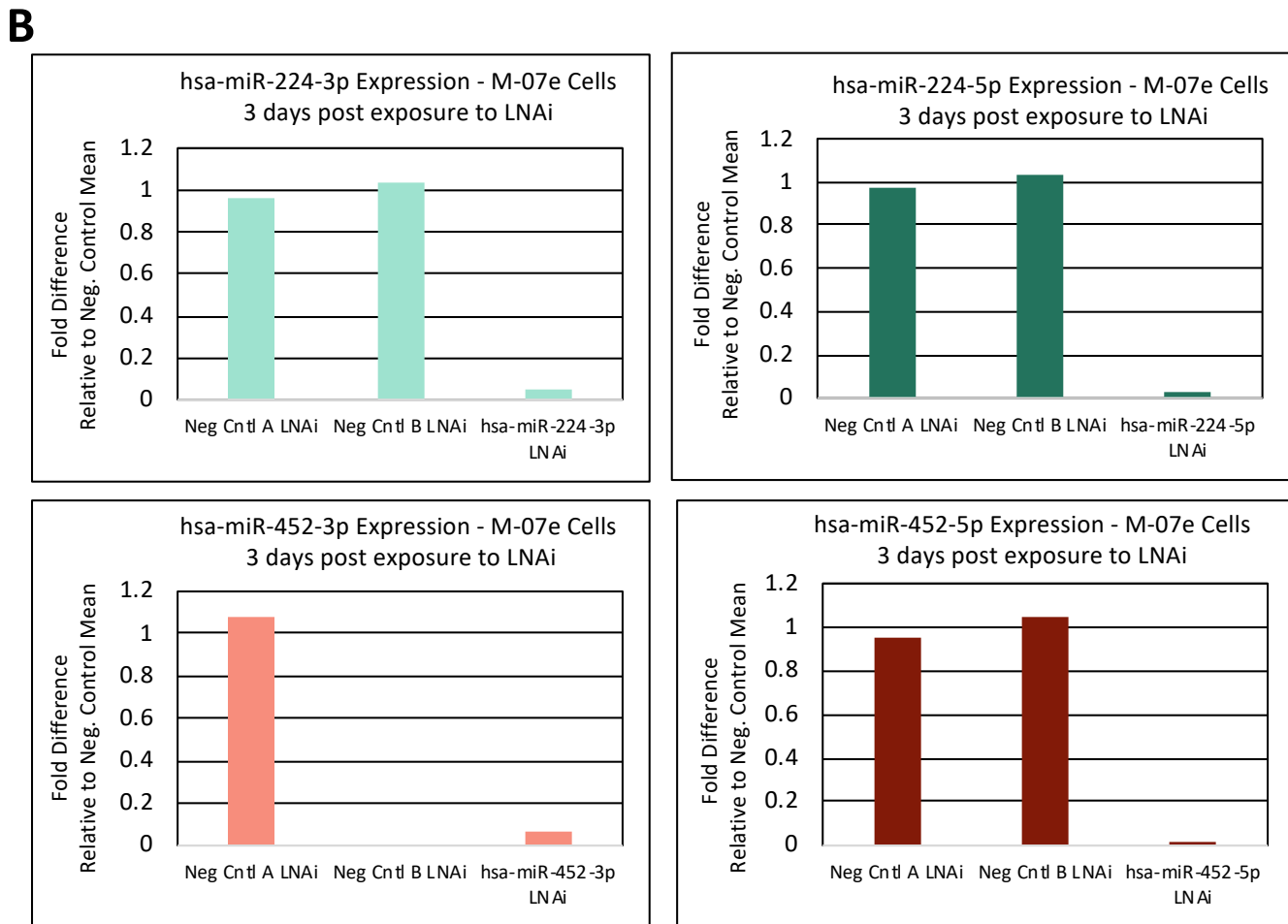
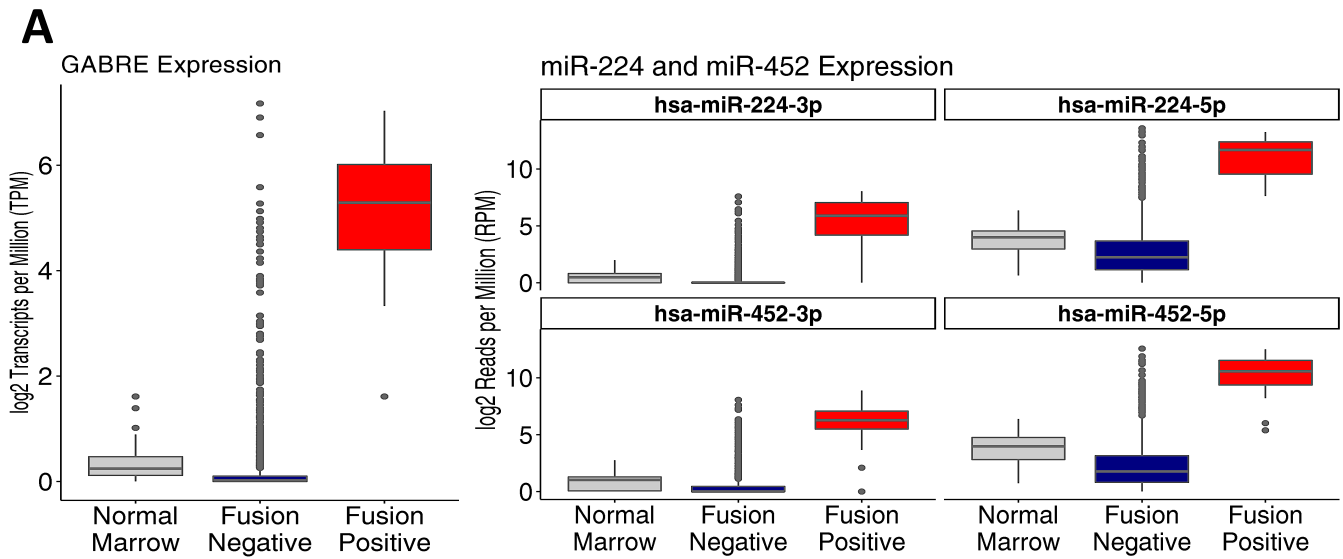


**Supplemental Figure 6. *CBFA2T3-GLIS2* confers enhanced proliferative potential in long-term culture of cord blood cells.** **A)** Transduced human CD34<sup>+</sup> cord blood stem cells (CBSC) with a lentivirus encoding the *CBFA2T3-GLIS2* fusion transcript and GFP (red) showed increased cumulative cell number compared to mock control (blue). **B)** Proportions of GFP<sup>+</sup> and CD34<sup>+</sup> cells are shown for *CBFA2T3-GLIS2*<sup>+</sup> cultures and mock control. Error bars denote standard deviation of duplicates.

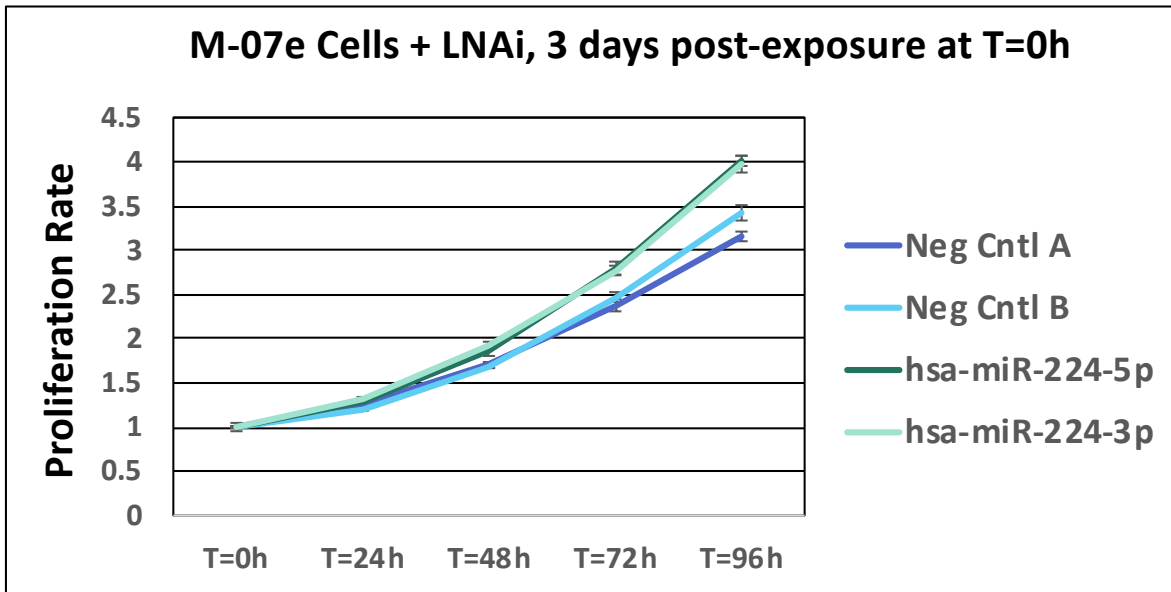
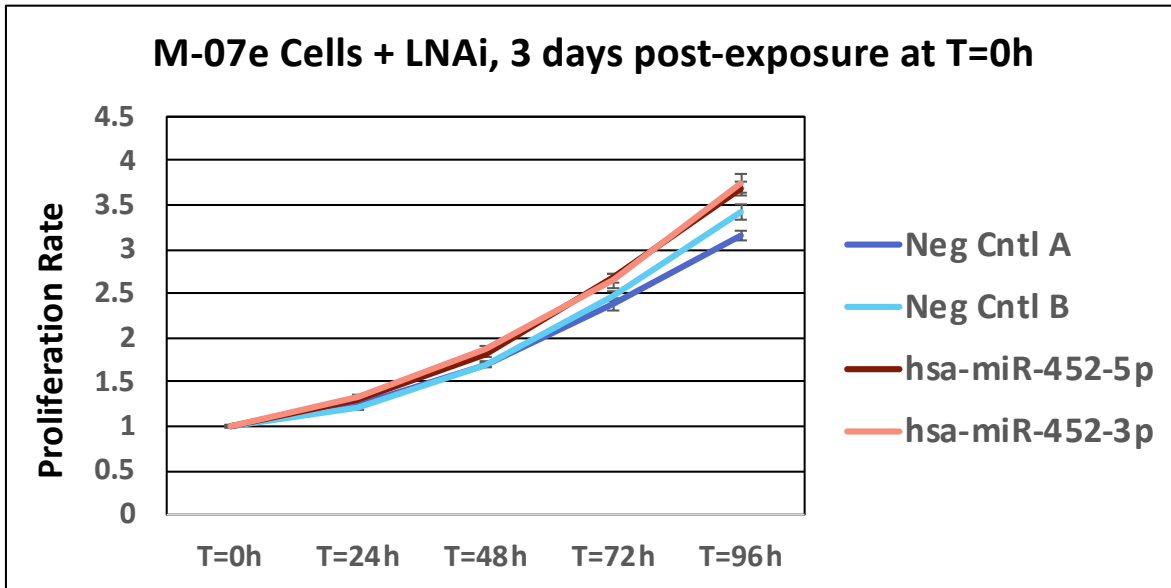
## Cell Adhesion and Cell-Surface Associated Genes in *CBFA2T3-GLIS2* AML



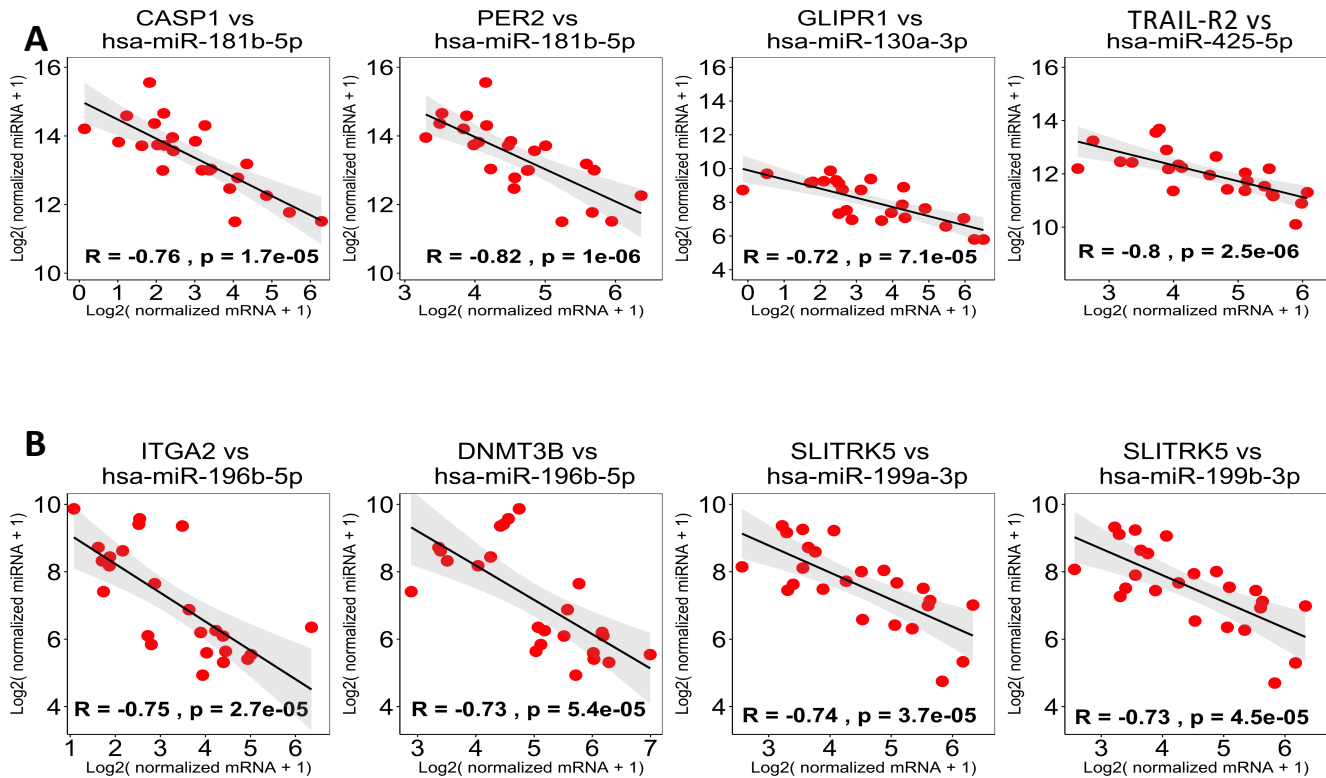
**Supplemental Figure 7. *CBFA2T3-GLIS2* patients highly over-express cell surface, cell adhesion and extracellular matrix associated genes.** Unsupervised hierarchal clustering of 1,049 AML patients RNA-sequencing data. Gene included are significantly up-regulated cell surface, cell-adhesion, and extracellular matrix gene markers in *CBFA2T3-GLIS2* AML (789 genes with  $\log_2$  old-change  $> 1.0$  and  $FDR < 0.001$ ). Color bars indicate primary cytogenetic code, M7 AML classification, fusion status (*CBFA2T3-GLIS2* in red), and trisomies associated with *CBFA2T3-GLIS2*. Labeled genes are highly over-expressed members of TGFB/BMP, Hedgehog, and NCAM1 interaction pathways (*BMP2*, *HHIP*, *NCAM1* and *CACNB2*), as well as two gene targets (*SLITRK5* and *GABRE*) with miRNA associations.



**Supplemental Figure 8. Efficiency of LNA Knockdown of miR-224 and miR-452 microRNAs in MO7E cell-lines.** **A)** *CBFA2T3-GLIS2* fusion-positive primary patient samples have increased transcript expression of *GABRE*, and the mature miRNAs *miR-224* and *miR-452*, which are transcribed from *GABRE* intronic regions. **B)** Knockdown of *miR-224-5p/3p* and *miR-452-5p/3p* expression by LNA miRNA inhibitors resulted in > 90% knockdown efficiency at 72 hours post-exposure measured by quantitative PCR.

**A****B**

**Supplemental Figure 9. LNA Knockdown of miR-224 and miR-452 shows a subtle increase in proliferation in MO7E cells.** A) Proliferation rates of *CBFA2T3-GLIS2* positive MO7E cultures were assessed for 4 days following exposure to LNA miRNA inhibitors directed against *hsa-miR-224-5p* or *hsa-miR-224-3p*, as well as B) *hsa-miR-452-5p* or *hsa-miR-452-3p*. Proliferation rates in knockdown conditions were compared to negative control A ( $p=0.001$ ) and control B ( $p=0.009$ ) after 96-hours.



**Supplemental Figure 10. MicroRNA-mRNA interactions in *CBFA2T3-GLIS2* AML involved with tumor suppressor and apoptotic functional roles.** Scatter plots of mRNA-miRNA interacting partners demonstrating anti-correlation of expression for **A)** apoptotic and tumor suppressor genes identified as significantly down-regulated in *CBFA2T3-GLIS2* AML with the over-expressed miRNAs, or **B)** significantly down-regulated tumor suppressor miRNAs whose gene partners were significantly up-regulated in the fusion-positive cohort.